IEEE Access
Multidisciplinary ⋮ Rapid Review ⋮ Open Access Journal

Received 27 December 2022, accepted 14 February 2023, date of publication 23 February 2023, date of current version 1 March 2023.

Digital Object Identifier 10.1109/ACCESS.2023.3248072

RESEARCH ARTICLE

Spectral Characteristics of DC Short Glow Discharge Plasma With Grid Electrodes

SHIXIN ZHAO[1], XINGBAO LYU[1], YANGGUO LIU[1], CHENGXUN YUAN[1,2], SVETLANA AVTAEVA[1,2,3], (Member, IEEE), ANATOLY KUDRYAVTSEV[1,2,4], XIAOXUE LI[1], JINGFENG YAO[1], YING WANG[1], AND ZHONGXIANG ZHOU[1,2]

[1]School of Physics, Harbin Institute of Technology, Harbin 150001, China
[2]Heilongjiang Provincial Key Laboratory of Plasma Physics and Application Technology, Harbin 150001, China
[3]Institute of Laser Physics SB RAS, 630090 Novosibirsk, Russia
[4]Physics Department, Saint Petersburg State University, 198504 Saint Petersburg, Russia

Corresponding authors: Xingbao Lyu (lyu_xingbao@163.com) and Chengxun Yuan (yuancx@hit.edu.cn)

This work was supported in part by the National Natural Science Foundation of China (NSFC) under Grant 12175050 and Grant 12205067, and in part by the Fundamental Research Funds for the Central Universities under Grant HIT.OCEF.2022036.

ABSTRACT The characteristics of post-cathode plasma maintained by a self-made DC short glow-discharge plasma generator with grid electrodes were measured by optical emission spectroscopy. The discharge existed in an abnormal glow discharge mode at a voltage of 250-400 V and a helium pressure of 3-15 Torr and a discharge gap of 3 mm. The results indicate that the intensity distribution of helium atom spectral lines in the post-cathode space differs from that in the post-anode space. The temperature of electron excitation in the post-cathode plasma reaches its peak of 1500-3000K at 5-6 mm from the grid cathode. The difference in the intensity distributions of helium atom spectral lines in the post-cathode and post-anode spaces is associated with electron generation mechanism in these cases.

INDEX TERMS Glow discharge, grid anode, spectral characteristics, post-anode plasma, effective thickness of plasma.

I. INTRODUCTION

The glow discharge plasma sources with a small electrode gap and a grid anode have been developed and studied for several decades because of their ability to generate plasma with parameters that are promising for a number of applications such as pumping gas lasers, coating deposition, electromagnetic wave propagation controls, initiation of reactions, etc., [1], [2], [3], [4], [5], [6], [7], [8]. In the process of glow discharge, positive column region is generally not available, but cathode falling region emerges a large electric field sufficient to generate runaway electrons, which, however, needs to satisfy the Dreicer criterion [9] expressed as $(E/p) > (E/p)_{cr}$, where E is the field intensity, and p is the gas pressure. In this case, electrons can enter a mode of continuous acceleration (runaway) because they acquire more energy than lose due to collisions. For helium $(E/p)_{cr} = 31\,\mathrm{V/(Pa \cdot m)}$, the mode of continuous acceleration can be achieved in a cathode dark space [10]. The possibility of electrons being accelerated in strongly ionized plasma is a consequence of the rapid decrease in the frequency at which electrons collide with ions and other electrons as its velocity increases.

If the product of gas pressure p and distance l between electrodes is $< (pl)_{min}$ corresponding to the left branch of the Paschen curve, ''hampered'' discharge condition is achieved. Within that range of pl, the Dreicer criterion can be reached prior to gas breakdown with discharge voltage peaking from 10^4 V–10^5 V. In this case, if a grid anode is used with a sufficiently large area (drift space) behind it, then it is possible to recover a high current from the discharge in the form of an electron beam [5], [11]. There are a lot of research on the various configurations of grid anode glow discharge in recent decades, which have demonstrated the high efficiency of electron beam generation [5], [6], [7], [8], [10], [11], [12], [13].

The exit of a beam of high-energy electrons into the space behind the anode leads to the formation post-anode plasma

The associate editor coordinating the review of this manuscript and approving it for publication was Xue Zhou.

with a sufficiently high electron number density. In addition, high-energy electron beams are capable of initiating various reactions in the region behind the anode, up to nuclear reactions [14]. The research interest in such discharge obviously is not weakened [15], [16], [17], [18], [19], [20], [21]. Yuan et al. simulated an electron beam generated by a glow discharge with grid anode [4], [22] and found that a DC glow discharge with grid anode could be used as part of a larger coating mounted on an aircraft to provide a plasma envelope that could be turned on and off.

The characteristics of post-anode plasma generated by glow discharge with grid anode and the efficiency and mechanism of electron beam generation have been studied by many research teams, However, there is little research on the distribution of electron number density and changing electron energy in the post-anode space [14].

Akishev and Dyatko investigated the characteristics of a strongly abnormal glow discharge with grid anode in inert gases at medium pressures used to obtain fast electrons in the kilovolt energy range [14]. as well as the active medium excited by fast electrons in the post-anode space after helium discharge spectroscopically at a pressure of 10 Torr–70 Torr. A pulse voltage of 1.5 kV–2 kV with a pulse duration of 10^{-3} s–10^{-1} s was applied to electrodes for discharge. Simulation by the Monte Carlo method allowed the authors to obtain the electron energy distribution function (EEDF) immediately behind the grid anode and to calculate the intensity of electron-ion pair generation and electronic level excitation as well as their dependence on distance from the grid anode.

This work focuses on a large-area DC grid anode glow discharge in helium at a pressure of 2 Torr–50 Torr and voltage of up to 1500 V [23]. It is concluded in this work that discharge behavior is typical for anomalous glow discharge. Using microwave diagnostic methods, it is found that electron density n_e is about 2×10^{9} cm^{-3}–6×10^{10} cm^{-3} and increases with the decrease in helium pressure and the rise of discharge current. The ionization degree is about 10^{-7}–10^{-6}, and the maximum attenuation of 10 GHz microwave radiation peaks at around 6% at a helium pressure of 2 Torr.

On this basis, the characteristics of DC short glow discharge between grid anode and solid-plate cathode are studied, together with two others electrode structures [24]. The results reveal that glow discharge with grid anode violates the Paschen's law. The minimum breakdown voltage on the experimental Paschen curves is greater than the theoretical value, and the slope of the right branch of the experimental Paschen curve is different from that of the theoretical curve, the shorter the electrode gap, the greater the slope of the right branch of the Paschen curve, and the left branch of the Paschen curve gradually shifts to the left. Based on the characteristics of short glow discharge, this work proposes a modified Paschen's law to effectively approximate the experimentally obtained Paschen curves.

Our previous work focused on the spectral characteristics of short glow discharge with grid electrodes in helium both in the electrode gap and in the space behind the grid anode [25]. Using the intensity distributions of helium atom spectral lines behind grid anode, we estimated the effective penetration thickness of the electrons penetration in the post-anode space to be about 10 mm–14 mm for short glow discharge with an inter-electrode gap of 1 mm–5 mm. We also explored the current-voltage characteristics of discharge and found that discharge existed in an abnormal glow discharge at a voltage of 250 V–400 V. However, discharge gap was found to decrease dramatically and remained unstable at a voltage of more than 400 V, resulting in filamentous discharge between electrodes, with no plasma generated in the post-electrode space.

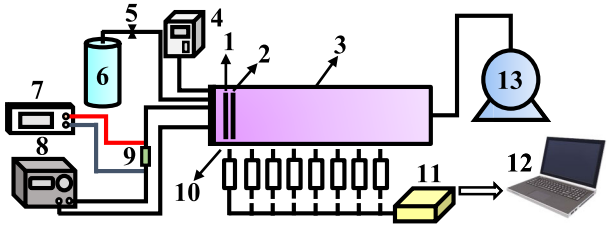

FIGURE 1. The DC discharge device with grid electrode. 1 – grid anode, 2 – grid cathode, 3 – fused silica tube, 4 - vacuum gauge, 5 - micro-metering valve, 6 -gas cylinder, 7 - oscilloscope, 8 - DC power supply, 9 - resistance, 10 - spectrometer probe, 11 -spectrometer, 12 - computer, 13 - vacuum pump.

The results presented in this article are a continuation of the studies carried out in [25]. The influence of helium pressure on the spectral characteristics of short glow discharge with grid electrode and the temperature distribution for electrons to be excited both in the electrode gap and in the space behind grid cathodes are investigated in this work. The research to be of interest for both possible applications and theoretical description of the post-cathode plasma generated by short glow discharges with grid cathode.

II. EXPERIMENTAL SETUP

The schematic diagram of DC discharge plasma generator with grid electrode is shown in Fig. 1. The device is composed of a discharge tube with two grid electrodes, digital DC regulated power supply, vacuum pump, helium bottle, etc.

Two grid electrodes were used as positive and negative electrodes respectively. The hole in anode was to facilitate the flow of working gas into discharge tube, and that in cathode was to enable charged particles in the discharge gap to pass through grid holes in cathode into the space behind the cathode (post-cathode space). The parameters of discharge tube and grid electrodes are specifically displayed in Table 1.

Prior to discharge, the discharge tube was pumped by vacuum pump to air pressure less than 5 Pa and then helium was fed into the tube with a fine-tuning valve to a pressure of several Torr to ensure that the purity of the working gas in the discharge tube was greater than 99.5%.

The DC power supply was intended to provide a stable voltage for discharge. The DC voltage used for discharge supply was 300 V. An RXG201 high-power corrugated resistor was

TABLE 1. Parameters of discharge tube and grid electrodes.

Parameter	Value
Length of discharge tube	150 mm
Outer diameter of discharge tube	30 mm
Inner diameter of discharge tube	25 mm
The electrode diameter	24 mm
The thickness of the electrode	1 mm
Diameter of support hole	6 mm
Grid hole diameter	4 mm
Discharge tube material	quartz
Number of holes in the cathode	8
Number of holes in the anode	4
Electrode materials	Pure iron

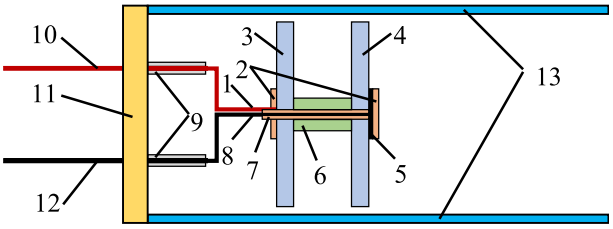

FIGURE 2. Schematic diagram of circuit connection in the discharge tube. 1 - wire connected to the anode, 2 - polytetrafluoroethylene nut, 3 - anode, 4 - cathode, 5 and 6 - polytetrafluoroethylene shims, 7 - hollow polytetrafluoroethylene stud, 8 - wire connected to the cathode, 9 - insulating layer, 10 - power feedthrough connected to the anode, 11 - discharge tube joint flange, 12 -connection to the cathode, 13 - discharge tube.

introduced into the circuit to prevent power supply damage and glow discharge from being converted into arc discharge.

Fig. 2 is a schematic diagram of the connection between two grids and power supply. The cathode and anode were fixed in the discharge glass tube by using a hollow polytetrafluoroethylene (PTFE) column.

The distance between the electrodes and the chosen constant voltage U_0 was designed to provide a cathode drop for charged particles to acquire energy and then to rapidly enter the post-electrode space, where they would lose energy along with gas ionization, thus generating plasma outside the electrode gap. The ions eventually bombarded the cathode surface and generate secondary electrons, required to sustain discharge.

The plasma emission intensity was measured by a fiber optic probe with a numerical aperture of 0.22 and transmitted to the entrance slit of the HR2000 spectrometer with an optical resolution of up to 0.065 nm (FWHM). All the collected spectra were digitally recorded in a computer by the same acquisition time, i.e. ten seconds.

III. EXPERIMENTAL RESULTS AND DISCUSSION

A. VOLT-AMPERE CHARACTERISTICS

The current-voltage characteristics of DC discharge with grid electrode have been studied early and presented elsewhere [25]. The discharge wa found to be in an abnormal glow discharge mode at a voltage of 250 V–400 V. When the discharge was maintained at these voltages, the glow of post-anode plasma could be observed with the naked eye behind the grid anode. The discharge gap decreased

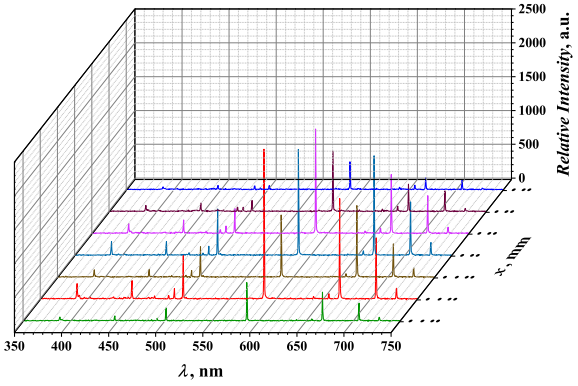

FIGURE 3. Spectra of DC glow discharge in helium obtained at different locations from the outer surface of grid cathode.

dramatically and remained unstable at a voltage of more than 400 V, resulting in filamentous discharge between electrodes with no plasma generated in the post-anode space. As short glow discharge between grid electrodes remained stable at a voltage of 275 V to 400 V, we used a direct voltage of 300 V to sustain glow discharge and generate plasma in the post-cathode space in this work. The experimental setup in this work was the same as that in [25], except that power supply poles were wrapped when connected to electrodes. To put it simple, the electrode 2 was anode in [25] but cathode in this work, and electrode 1 in [25] was cathode but anode in this work.

B. EMISSION SPECTRUM OF DC GRID DISCHARGE PLASMA

Fig. 3 shows the emission spectra of the DC short glow discharge with grid electrodes in helium. Helium emitted from both discharge gap and post-cathode space during discharge. Negative values of the x-coordinate to regions in the space between electrodes, and positive values correspond to the region behind the grid cathode. Zero is located on the surface of the grid cathode from the side of the post-cathode space. The observed discharge emission was concentrated in the wavelength range of 350 nm to 750 nm.

As can be seen from the figure,, all the recorded spectra emitted both from the discharge gap and from the post-cathode space only involved helium atoms lines. Helium ion lines were not detected in the discharge spectra, nor was the radiation of possible impurities (nitrogen, oxygen, water vapor) in the spectra, which indicates a very low content of impurities in the gas inside the discharge device.

All the spectra of DC glow discharge in helium was made up of eight distinct atomic spectral lines, as presented in Table 2, together with their spectral parameters [26], [27].

C. AXIAL DISTRIBUTIONS OF DISCHARGE RADIATION INTENSITY

The axial distribution of discharge emission in the discharge gap and post-cathode space was examined at a discharge gap of 3 mm, a helium pressure of 15 Torr and a DC voltage of 300 V between grid electrodes. The measurements were

TABLE 2. Parameters of helium atom spectral lines.

Spectral wavelength (nm)	Electron configuration	Transition probability A ($10^7 s^{-1}$)	The excitation energy (eV)	Statistical weight
388.9	1s3p→1s2s	0.947	23.007	5
447.1	1s4d→1s2p	1.843	23.736	5
492.2	1s4d→1s2p	1.986	23.736	5
501.6	1s3p→1s2s	1.337	23.087	3
587.6	1s3d→1s2p	5.302	23.074	5
667.8	1s3d→1s2p	6.371	23.074	5
706.5	1s3s→1s2p	1.547	22.718	3
728.1	1s3s→1s2p	1.830	22.920	1

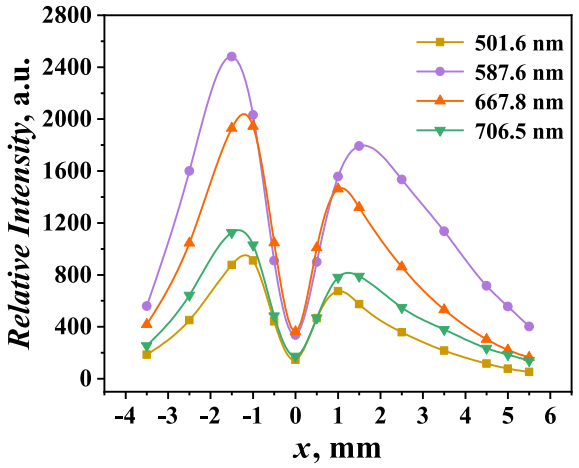

FIGURE 4. Axial distributions of discharge emission on different wavelengths.

respectively carried out on the wavelengths of helium atom spectral lines 501.6 nm, 587.6 nm, 667.8 nm and 706.5 nm, as shown in Fig. 4.

It can be seen from the figure that there were two peaks on the intensity distribution on all wavelengths, one of which was in the space between electrodes at a distance of 0.1 mm to 0.6 mm from the cathode ($x = -1.1$ mm to -1.6 mm; cathode thickness was 1 mm) and the other in the post-cathode space at a distance of 1.1 mm to 1.5 mm from the cathode. The emission spectral intensity of the space behind the cathode was of the same order of magnitude as that between the electrodes.

The maximum intensity in the space between electrodes corresponded to the negative glow area of discharge, therefore the length of the cathode sheath adjacent to the inner surface of the cathode did not exceed tenths of a millimeter. The absence of a radiation intensity saturation region behind the negative glow indicated that of a positive column, which is typical of short glow discharge [17].

It is of great importance to understand the reasons for the presence of a maximum intensity in the post-cathode space at a certain distance from the outer side of grid cathode. It would seem more reasonable to have a radiation maximum immediately behind the cathode and a gradual decrease in intensity with distance from the cathode. The presence of an intensity maximum in the post-cathode space at a certain distance from the cathode indicates the lack of electrons immediately

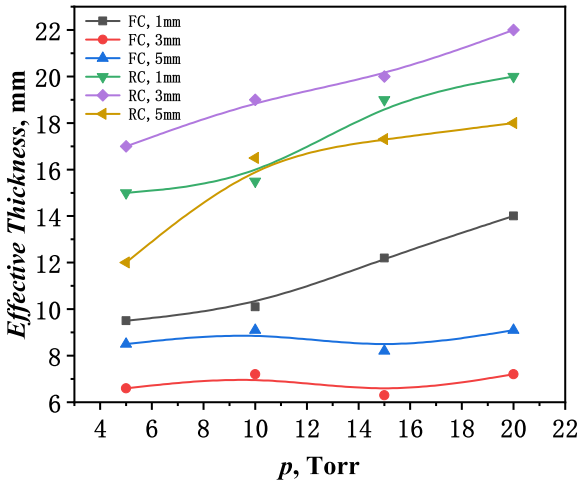

FIGURE 5. The effective post-cathode plasma thickness as function of helium pressure for the glow discharge with electrode gaps of 1, 3 and 5 mm. The effective post-anode plasma thickness is shown for comparison. The RC (Reverse Connection) means that electrode 1 is anode and electrode 2 is cathode, as shown in Fig. 1. The FC (Forward Connection) means that electrode 1 is cathode and electrode 2 is anode as in our previous study [25].

behind the cathode and their generation in the post-cathode space by an ion beam penetrating through holes in the cathode into the post-cathode space. This is a reasonable assumption since the cathode layer repels electrons and accelerates ions towards the cathode [28], [29]. Some of these accelerated ions penetrated through holes in the cathode into the space behind the cathode, forming a post-cathode plasma, the maximum density of which is at a certain distance from the cathode.

Another explanation for the presence of the intensity maximum at some distance from the cathode that it was potentially associated with opposite trends in the change in the density and temperature of electrons in the post-cathode space. In case that electron density continuously decreased with distance from the cathode, while electron temperature increased, then the maximum helium line was intensified at a certain distance from the cathode, which can be expressed by a function of both electron density and their temperature.

The axial distributions of discharge emission was employed to define the effective penetration thickness of electrons in the post-cathode space d_{eff} as the distance from the outer surface of the grid cathode to a position where the HeI lines emission was short enough, namely, their arbitrary intensity I decreased to $10Inoise$, where $Inoise$ is the mean intensity of noise $d_{eff} = x_{I=10Inoise}$.

The effective penetration thicknesses of electrons in the post-cathode space under different discharge conditions derived are shown in Fig. 5, together that in [25].

The reverse connection (RC) and forward connection (FC) in Fig. 5 individually correspond to the measured plasma thickness in the post-cathode and post-anode spaces.

As shown in Fig. 5, the effective thickness of plasma in the post-cathode for all the electrode gaps increased with the increase in helium pressure and reached its maximum

when electrode gap was 3 mm. The thickness of plasma in the post-cathode space was greater than the length of electron gap but smaller than that of plasma in the post-anode space. The difference in the effective thickness of plasma in the post-cathode and post-anode spaces was maximized when the length of electrode gap was 3 mm.

D. ELECTRON EXCITATION TEMPERATURE

In the case of the Boltzmann distribution of excited atoms over energy levels, the number density of atoms in the excited and ground states is related by [30]:

$$N_k = N_0(\frac{g_k}{g_0})\exp(-\frac{E_i}{k_B T_{ex}}), \tag{1}$$

where N_k and N_0 are number densities of atoms in excited and ground states, g_k and g_0 are the degeneracy of the energy level, E_i is excitation energy, T_{ex} is electron excitation temperature and k_B is Boltzmann constant.

Hence, the intensity of spectral line is given by:

$$I_{ki} \sim (\frac{hc}{\lambda_{ki}})A_{ki}N_0(\frac{g_k}{g_0})\exp(-\frac{E_i}{k_B T_{ex}}), \tag{2}$$

where A_{ki} is transition probability, λ_{ki} is line wavelength, c and h are known constants.

The electronic excitation temperature can be found from the slope of the semilogarithmic dependence of the reduced intensity of the spectral lines $(I_{ki}\lambda_{ki})/(g_k A_{ki})$ on the energy of the upper state of the spectral transition E_i:

$$L_n\frac{I_{ki}\lambda_{ki}}{g_k A_{ki}} \sim -\frac{E_i}{k_B T_{ex}}. \tag{3}$$

We used this relation to determine electron excitation temperature in the post-cathode plasma of short glow discharge.

The axial distribution of electron excitation temperature at distances of 1 mm–10 mm from the outer surface of grid cathode was measured at a discharge gap of 3 mm and a helium pressure of 15 Torr. The effect of helium pressure on electron excitation temperature at 1.5 mm from the outer surface of grid cathode was also explored.

Compared with the information-rich atomic and molecular spectra such as argon, oxygen and nitrogen, the number of characteristic spectral lines in the helium discharge spectra was relatively small, which, therefore, could be used to measure electron excitation temperature in the helium plasma. Five spectral lines of helium atoms with wavelengths of 388.9 nm, 728.1 nm, 447.1 nm, 587.6 nm and 706.5 nm, having most large radiation intensity and different excitation energies were selected for the measurements. Parameters of these spectral lines are presented in Table 2.

Careful studies of scattering the experimental points of the dependence of $L_n(I_{ki}\lambda_{ki})/(g_k A_{ki})$ on E_i showed that it would be the most effective to measure electron excitation temperature using three wavelengths of 447.1 nm, 587.6 nm and 706.5 nm as an error of the dependence fitting by a straight line in this case is minimal. The measurement results of electron excitation temperature from these three spectral lines are shown in Fig. 6, together with the results of fitting the dependence of $L_n(I_{ki}\lambda_{ki})/(g_k A_{ki})$ on E_i calculated from the measured intensities of helium lines in the post-cathode space at various distances from the cathode.

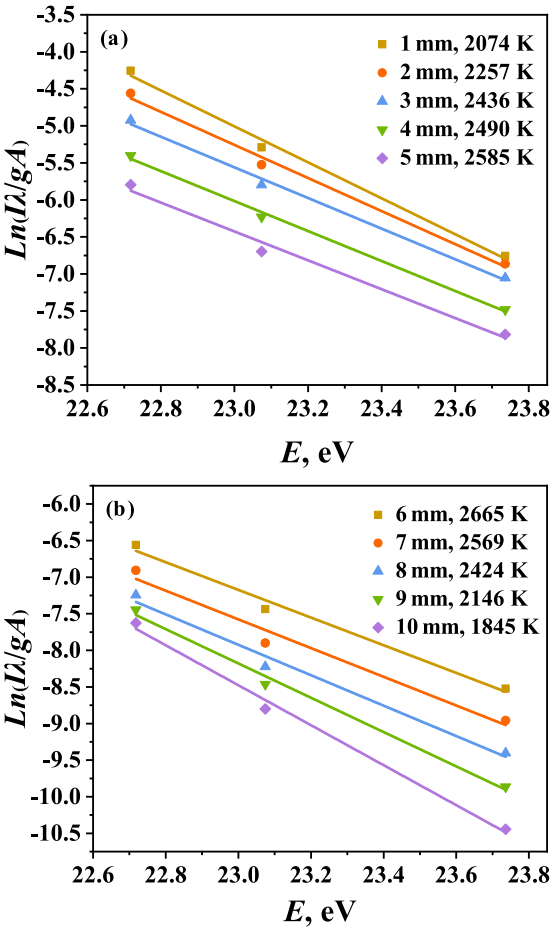

FIGURE 6. Fitting straight lines for calculating the electron excitation temperatures of helium discharge plasma at different distances from the grid cathode; a) 1-5 mm, b) 6-10 mm.

The axial distribution of electron excitation temperature in the post-cathode space at distances of 1 mm–10 mm from the cathode, measured at a discharge gap of 3 mm and a helium pressure of 15 Torr, is shown in Fig. 7. As obviously shown in the figure, electron excitation temperature at 1 mm from the cathode was about ~2000 K and firstly increased with the distance from the cathode, reaching its maximum at about 2650 K at distances of 5 mm–7 mm, and then decreased to about 1850 K at a distance of 10 mm from the cathode.

In equilibrium, the temperature at which the electron is excited is equal to the temperature of the electron. In non-equilibrium conditions, the temperature of electron excitation may be different from that of the electron; nevertheless, its change reflects changing trend of the change in the electron temperature. Therefore, we concluded that electron temperature also increased with distance from the cathode, reaches a maximum at a certain distance, and then decreases. The initial increase in the electron temperature in the post-cathode space

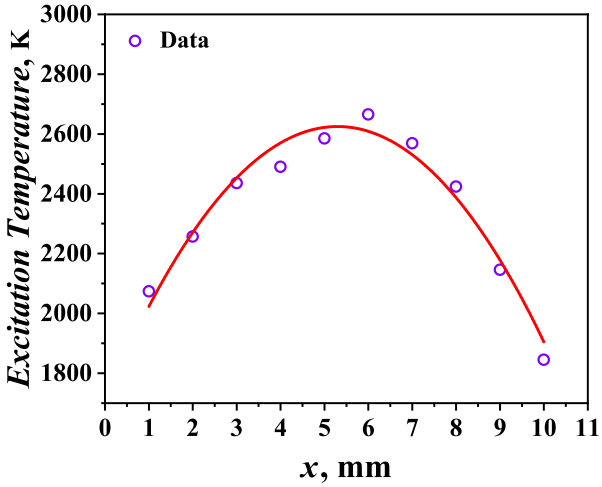

FIGURE 7. The electron excitation temperature in post-cathode space as a function of distance from cathode.

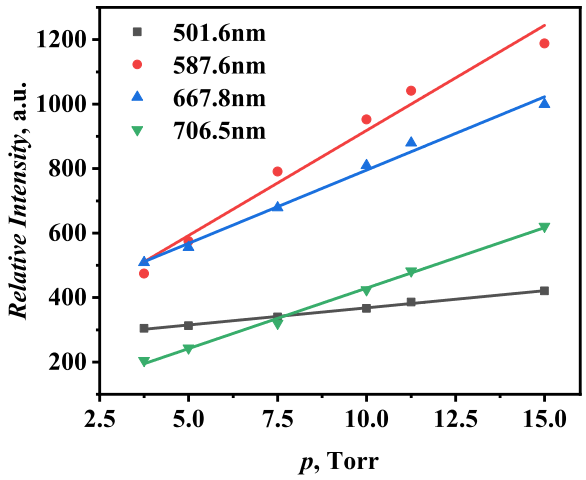

FIGURE 8. The dependence of HeI spectral line intensity in the space behind the grid cathode at distance of 2mm from the cathode on helium pressure; discharge gap was 1mm.

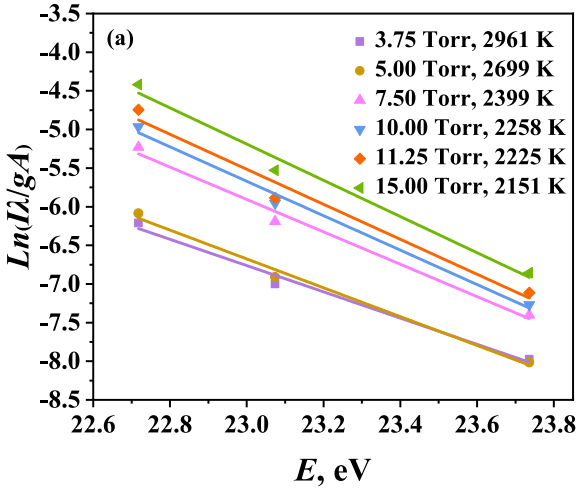

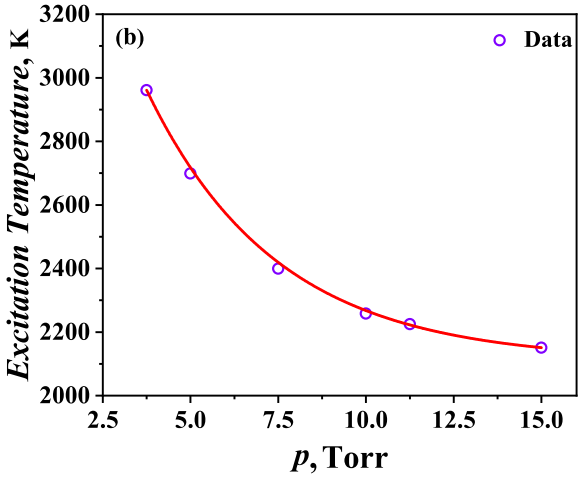

FIGURE 9. (a) Fitting straight lines for calculating the electron excitation temperatures; (b) The electron excitation temperature as a function on pressure.

is apparently associated with the need to generate plasma under conditions of decreasing electron density, however, starting from a certain distance from the cathode, the field due to the space charge of the post-cathode plasma weakens and the electron temperature begins to decrease.

The above changing trend in the electron temperature of plasma in the post-cathode space with distance from the cathode explains the presence of a maximum intensity of helium lines at a distance of about 1 mm–1.6 mm from the cathode.

E. EFFECT OF PRESSURE EFFECT ON HELIUM LINE INTENSITIES AND ELECTRON EXCITATION TEMPERATURE IN THE POST-CATHODE SPACE

The dependence of HeI spectral line intensity in the space behind the grid on helium pressure was studied in the helium pressure range of 3 mm–15 mm. Typical dependence is shown in Fig. 8.

As can be seen from Fig. 8, the intensity of the HeI spectral lines in the post-cathode space increased linearly with the increase in helium pressure. Apparently, which apparently indicates that helium atoms in the post-anode space were excited by direct electron impact when electrons collided with helium atoms in the ground state. The number density of neutral atoms $n_g = p/(k_B T_g)$ increased with the increase of helium pressure P, and the mean free path of electrons $\lambda_R = 1/(n_g \sigma)$ became smaller (k_B is the Boltzmann constant, T_g is the gas temperature of the plasma, σ is the collision cross section of charged particles). As a result, the collision frequency between electrons and neutral atoms $v_{en} = n_g \sigma v$ increased, so did the excitation rate of atoms (v is the electron velocity). And eventually the radiation intensity of spectral lines increased with the increase of helium pressure.

Hence, we concluded that there were electrons with a sufficiently high density in the post-cathode space to excite helium atoms at the energy level.

In addition, the effect of helium pressure on the temperature of electronic excitation in the post-cathode space was studied. The measurements were carried out at a discharge gap of 3 mm at a distance $x = 1.5$ mm from

the outer surface of grid cathode. The helium pressure varied from 3.5 Torr–15 Torr.

The dependence of $Ln(I_{ki}\lambda_{ki})/(g_kA_{ki})$ on E_i for HeI line intensity at various helium pressures is shown in Fig. 9(a) and that of electron excitation temperature on pressure is shown in Fig. 9(b). It can be seen from the figures that in the pressure range of 3.75 Torr–15 Torr, the electronic excitation temperature of helium plasma in the post-cathode space gradually decreased with the increase of pressure because with the increase of the probability of recombination between electrons and ions, the number of neutral atoms increased, and mean free path became smaller, the number of effective collisions between electrons and neutral atoms and the energy loss increased, which further led to the decrease of electron energy [29].

IV. CONCLUSION

The characteristics of helium plasma maintained with a home-made DC glow discharge plasma generator with grid electrodes were measured by optical emission spectroscopy.

The obtained emission of helium plasma is mainly concentrated in the wavelength range of 350 nm–750 nm, and all lines of the spectra are HeI lines. The intensity of spectral lines in the post-cathode space during discharge is obviously stronger than that in the post-anode space, and reaches its maximum in the discharge gap at a distance about 1 mm–1.6 mm from grid cathode. In the space behind grid cathode, the radiation intensity of HeI spectral lines is maximized at a certain distance from the grid cathode, which is different from that in the post-anode space where HeI line intensity decreases with distance from the grid anode [25]. Both in the discharge gap and in the space behind the electrode, the intensity of spectral lines increases with the increase of pressure.

For all electrode gaps, the thickness of plasma in the post-cathode space increases with helium pressure and is greater than that of plasma in the post-anode space.

The electron excitation temperature in the post-cathode space was calculated from the slope of the Boltzmann dependence of $Ln(I_{ki}\lambda_{ki})/(g_kA_{ki})$ on E_i. The electron excitation temperature reaches its maximum at a distance about 5 mm–6 mm from cathode and decreases with the increase in helium pressure. The electron excitation temperature at a discharge voltage of 300 V and a helium pressure of 3 Torr–15 Torr was 1500 K–3000 K.

The difference in intensity distribution observed in the post-anode and post-cathode spaces is caused by the fact that plasma is generated by a beam of runaway electrons in the post-anode space, whose intensity and energy decrease with distance from the grid anode. In the case of post-cathode plasma, the accelerated ions in the cathode sheath fly to the post-cathode space, causing secondary ion emission of electrons on the outer surface of the grid cathode and redistribution of the electric field in the post-cathode space. Secondary electrons are accelerated by an electric field in the direction from the cathode, and only after acquiring necessary energy do they become able to excite and ionize helium atoms. Therefore, electron excitation temperature and spectral line intensity are maximized at a certain distance from grid cathode.

REFERENCES

[1] K. Yi, D. Liu, X. Chen, J. Yang, D. Wei, Y. Liu, and D. Wei, "Plasma-enhanced chemical vapor deposition of two-dimensional materials for applications," *Accounts Chem. Res.*, vol. 54, no. 4, pp. 1011–1022, Feb. 2021.

[2] I. Adamovich et al., "The 2017 plasma roadmap: Low temperature plasma science and technology," *J. Phys. D, Appl. Phys.*, vol. 50, no. 32, 2017, Art. no. 323001.

[3] G. S. Oehrlein and S. Hamaguchi, "Foundations of low-temperature plasma enhanced materials synthesis and etching," *Plasma Sources Sci. Technol.*, vol. 27, no. 2, Feb. 2018, Art. no. 023001.

[4] C. Yuan, R. Tian, S. I. Eliseev, V. S. Bekasov, E. A. Bogdanov, A. A. Kudryavtsev, and Z. Zhou, "Numerical simulation and analysis of electromagnetic-wave absorption of a plasma slab created by a direct-current discharge with gridded anode," *J. Appl. Phys.*, vol. 123, no. 11, Mar. 2018, Art. no. 113303.

[5] J. J. Rocca, J. D. Meyer, M. R. Farrell, and G. J. Collins, "Glow-discharge-created electron beams: Cathode materials, electron gun designs, and technological applications," *J. Appl. Phys.*, vol. 56, no. 3, pp. 790–797, Aug. 1984.

[6] P. A. Bokhan and D. E. Zakrevsky, "Self-sustained photoelectron discharge," *Appl. Phys. Lett.*, vol. 81, no. 14, pp. 2526–2528, Sep. 2002.

[7] S. G. Belostotsky, D. V. Lopaev, Y. A. Mankelevich, E. A. Muratov, A. T. Rakhimov, V. B. Saenko, and M. A. Timofeev, "Light efficiency of cathodoluminescent screens excited by a runaway electron beam," *Plasma Phys. Rep.*, vol. 34, no. 11, pp. 969–977, Nov. 2008.

[8] R. Gao, C. Yuan, S. Liu, F. Yue, J. Jia, Z. Zhou, J. Wu, and H. Li, "Broadband microwave propagation in a novel large coaxial gridded hollow cathode helium plasma," *Phys. Plasmas*, vol. 23, no. 6, Jun. 2016, Art. no. 063304.

[9] H. Dreicer, "Electron and ion runaway in a fully ionized gas. I," *Phys. Rev. J. Arch.*, vol. 115, no. 2, p. 238, 1959.

[10] P. A. Bokhan and A. R. Sorokin, "Gas laser excitation by an electron beam formed at open discharge," *Opt. Quantum Electron.*, vol. 23, no. 4, pp. S523–S538, 1991.

[11] A. I. Golovin, E. K. Egorova, and A. I. Shloido, "Estimation of the current-voltage characteristic of an open discharge," *Tech. Phys.*, vol. 59, no. 10, pp. 1445–1451, Oct. 2014.

[12] R. Gao, C. Yuan, H. Li, J. Jia, Z.-X. Zhou, J. Wu, Y. Wang, and X. Wang, "Absolute continuum intensity diagnostics of a novel large coaxial gridded hollow cathode argon plasma," *Phys. Plasmas*, vol. 23, no. 8, Aug. 2016, Art. no. 083525.

[13] Y. Liang, C. Yuan, R. Gao, J. Jia, G. Kirsanov, V. Bekasov, A. Marin, A. Kudryavtsev, S. Eliseev, and Z. Zhou, "Investigation of low-pressure glow discharge in a coaxial gridded hollow cathode," *IEEE Trans. Plasma Sci.*, vol. 44, no. 12, pp. 2965–2972, Dec. 2016.

[14] A. N. P. P. Y. S. Akishev and N. A. Dyatko, "Abnormal smoldering discharge in dense gases as a stachionary source of fast electrons of kilowatt range," *ZhTF*, vol. 59, no. 8, p. 14, 1989.

[15] J. Jia, C. Yuan, A. Kudryavtsev, S. Eliseev, G. Kirsanov, V. Bekasov, R. Gao, and Z. Zhou, "Numerical and experimental diagnostics of dusty plasma in a coaxial gridded hollow cathode discharge," *IEEE Trans. Plasma Sci.*, vol. 44, no. 12, pp. 2973–2978, Dec. 2016.

[16] C. Yuan, J. Yao, S. I. Eliseev, E. A. Bogdanov, A. A. Kudryavtsev, and Z. Zhou, "On self-sustainment of DC discharges with gridded anode," *J. Appl. Phys.*, vol. 122, no. 14, Oct. 2017, Art. no. 143304.

[17] A. A. Kudryavtsev, A. V. Morin, and L. D. Tsendin, "Role of nonlocal ionization in formation of the short glow discharge," *Tech. Phys.*, vol. 53, no. 8, pp. 1029–1040, 2008.

[18] I. Rafatov, E. A. Bogdanov, and A. A. Kudryavtsev, "Account of nonlocal ionization by fast electrons in the fluid models of a direct current glow discharge," *Phys. Plasmas*, vol. 19, no. 9, Sep. 2012, Art. no. 093503.

[19] J. Gledhill, "The range-energy relation for 0.1–600 keV electrons," *J. Phys. A, Math., Nucl. Gen.*, vol. 6, no. 9, p. 1420, 1973.

[20] C. Yuan, A. A. Kudryavtsev, A. I. Saifutdinov, S. S. Sysoev, R. Tian, J. Yao, and Z. Zhou, "Probe diagnostics of plasma parameters in a large-volume glow discharge with coaxial gridded hollow electrodes," *IEEE Trans. Plasma Sci.*, vol. 45, no. 12, pp. 3110–3113, Dec. 2017.

[21] C. Yuan, A. A. Kudryavtsev, A. I. Saifutdinov, S. S. Sysoev, J. Yao, and Z. Zhou, "Diagnostics of large volume coaxial gridded hollow cathode DC discharge," *Plasma Sources Sci. Technol.*, vol. 28, no. 6, Jun. 2019, Art. no. 067001.
[22] S. I. Eliseev, E. A. Bogdanov, and A. A. Kudryavtsev, "Slow electron energy balance for hybrid models of direct-current glow discharges," *Phys. Plasmas*, vol. 24, no. 9, Sep. 2017, Art. no. 093503.
[23] X. Lyu, C. Yuan, S. Avtaeva, A. Kudryavtsev, J. Yao, Z. Zhou, and X. Wang, "A large-area DC grid anode glow discharge in helium," *Plasma Phys. Rep.*, vol. 47, no. 4, pp. 369–376, Apr. 2021.
[24] X. Lyu, C. Yuan, S. Avtaeva, A. Kudryavtsev, J. Yao, Z. Zhou, and X. Wang, "Paschen curves and current–voltage characteristics of large-area short glow discharge with different electrode structures," *Phys. Plasmas*, vol. 27, no. 12, Dec. 2020, Art. no. 123509.
[25] X. Lyu, C. Yuan, S. Avtaeva, A. Kudryavtsev, J. Yao, Y. Liu, Z. Zhou, and X. Wang, "Spectral characteristics of a short glow discharge with a grid anode," *AIP Adv.*, vol. 12, no. 3, Mar. 2022, Art. no. 035202.
[26] A. Kramida, Y. Ralchenko, J. Reader, and NIST ASD Team, "NIST atomic spectra database (ver. 5.8)," Nat. Inst. Standards Technol., Gaithersburg, MD, USA, 2020. Accessed: May 17, 2021. [Online]. Available: https://physics.nist.gov/asd
[27] N. Bibinov, A. Fateev, and K. Wiesemann, "Variations of the gas temperature in He/N_2 barrier discharges," *Plasma Sources Sci. Technol.*, vol. 10, no. 4, p. 579, 2001.
[28] M. A. Lieberman and A. J. Lichtenberg, *Principles of Plasma Discharges and Materials Processing*. Hoboken, NJ, USA: Wiley, 2005.
[29] Y. P. Raizer and J. E. Allen, *Gas Discharge Physics*. Berlin, Germany: Springer, 1991, vol. 1.
[30] B. M. Smirnov, *Theory of Gas Discharge Plasma*. Cham, Switzerland: Springer, 2015.

SHIXIN ZHAO received the bachelor's degree in physics from Ludong University, China, in 2018. He is currently pursuing the Ph.D. degree with the Harbin Institute of Technology (HIT), China.

Since 2018, he has been with the School of Physics, (HIT). His research interests include atmospheric plasmoids, high-voltage discharges, and plasma diagnostics.

XINGBAO LYU received the Ph.D. degree in physics from the Harbin Institute of Technology (HIT), China, in 2022.

He is currently an Assistant Researcher with the School of Physics, HIT. His research interests include fundamental properties of atmospheric plasma and the interaction between plasma and electromagnetic waves.

YANGGUO LIU received the bachelor's degree in physics from the Shandong University of Technology, China, in 2019.

From 2019 to 2022, he was at the School of Physics, Harbin Institute of Technology, China. His research interest includes plasma spectral diagnostics.

CHENGXUN YUAN received the bachelor's and Ph.D. degrees from the Harbin University of Technology, China, in 2004 and 2011, respectively.

He is currently a Professor with the School of Physics, Harbin Institute of Technology. He has more than 200 publications in the plasma field. His research interests include basic plasma physics, dusty plasma physics, and the interaction of electromagnetic radiation with plasma.

SVETLANA AVTAEVA (Member, IEEE) received the Ph.D. degree in physico-mathematical science from Lomonosov's Moscow State University, Russia, in 2012.

Since September 2017, she has been a Senior Scientist with the Laboratory of Super-Short Laser Pulse Physics, Institute of Laser Physics SB RAS, Novosibirsk. She had published more than 150 papers in scientific journals, books and conference proceedings, and one monograph.

ANATOLY KUDRYAVTSEV received the M.S. and Ph.D. degrees in physics from Leningrad State University, Saint Petersburg, Russia, in 1976 and 1983, respectively.

Since 1982, he has been with Saint Petersburg State University, where he is currently an Associate Professor with the Department of Optics. He is an expert in the gas discharge physics and kinetic theory of plasma physics. He is the author of more than 100 journal articles and numerous conference presentations.

XIAOXUE LI received the bachelor's degree in physics from Harbin Normal University, China, in 2021.

Since 2021, she has been with the School of Physics, Harbin Institute of Technology, China. Her research interest includes characteristic of the post-cathode space plasma.

JINGFENG YAO was born in China, in 1994. He received the B.S. and Ph.D. degrees in physics from the Harbin Institute of Technology (HIT), Harbin, China, in 2021.

He is currently an Assistant Professor with the School of Physics, HIT. His current research interests include plasma diagnostics, fundamental study of plasma sources, gas discharges, and its application.

YING WANG was born in China, in 1985. She received the B.S. and Ph.D. degrees in physics from the Harbin Institute of Technology (HIT), Harbin, China, in 2013.

She is currently an Associate Professor with the School of Physics, HIT. Her research interests include basic plasma physics and interaction between laser beam and plasma.

ZHONGXIANG ZHOU received the B.S. degree in physics from Jilin University, Changchun, China, in 1987, and the Ph.D. degree in optics from the Harbin Institute of Technology (HIT), Harbin, China, in 1997.

Since 2000, he has been a Full Professor of physics with the Department of Physics, HIT. His research interests include electromagnetic-wave interactions with plasma, dusty plasma, and terahertz technology.